

Dynamic localization versus photon-assisted transport in semiconductor superlattices driven by dc-ac fields

W.-X. Yan^{1,2}, S.-Q. Bao^{1,3}, and X.-G. Zhao^{1,2,3}

¹*CCAST (World Laboratory) P.O. Box 8730, Beijing 100080, China*

²*Institute of Theoretical Physics, Academia Sinica, P.O. Box 2735, Beijing 100080, China*

³*Institute of Applied Physics and Computational Mathematics,*

P.O. Box 8009, Beijing 100088, China

Abstract

Via the numerical analysis on the intraband dynamics of optically excited semiconductor superlattices, we find that time-integrated squared THz emission signals can be used for probing both dynamic localization and multiphoton resonance in the coherent regime. Competition effect between dynamic localization and photon-assisted transport has also been discussed.

PACS numbers: 78.47.+p, 42.50.Md, 73.20.Dx, 78.20.Jq

Recently, semiconductor superlattices (SL) driven by external electric fields have been a subject of intensive investigations both theoretically and experimentally. The most significant example is Bloch oscillation (BO) which was theoretically predicted many years ago and experimentally demonstrated recently in SL driven by a uniform electric field. While, in the regime of tight-binding approximation, an intense laser field (ac fields) can make a charged particle localized around the initially injected place, which is the so-called dynamic localization [1]. Then the natural subsequent question will be the following: What will happen if the electrons in SL are subject to the combined dc-ac fields? Actually, this question is answered by the recent several theoretical predictions and experimental observations. For example, multi-photon absorption [2], absolute negative conductivity [3], photon-assisted transport [4], fractional Wannier-Stark ladders [5], etc. Particularly, the recent experiment on the multiple quantum-well superlattices driven by dc-ac fields has confirmed through probing the static I - V characteristics that the electrons in SL can tunnel through the adjacent wells through the stimulated emission and absorption of photons [4]. In this facet, the common action of the dc-ac field plays the constructive role on the transport properties in SL. However, the dc-ac field can also play the destructive role on the transport in SL, which can be manifested in dynamic localization induced by dc-ac fields, provided that the ratio of the Stark frequency $\omega_B (= eF_0d$, d is the SL lattice constant and F_0 is the amplitude of dc fields) to the ac field frequency ω is an integer n , and $edF_1/\hbar\omega$ (F_1 is the amplitude of ac fields) is a root of ordinary Bessel function of the order n : $J_n(edF_1/\hbar\omega) = 0$ [1]. In this case, the electrons will become localized. Hence, the effect from both dc and ac fields play the dual role in the transport properties in SL.

In the static regime, the usual method in the investigation of transport properties in SL under the influence of external fields is through the observation of static I - V characteristics [4]. In the realm of ultra-short laser pulse (usually in hundreds of femto-second duration) generated coherent regime, what physical quantity can be used to probe the transport properties induced by the external fields? This question was partially answered by T. Meier et al with the help of the well-known semiconductor Bloch equations [6]. They found by monitoring the time-integrated squared THz emission signals that even in the presence of excitonic interactions comparable to the miniband widths, the carriers driven by pure intense laser fields (ac fields) reveal dynamic localization provided that $edF_1/\hbar\omega$ coincides with the roots of the ordinary Bessel function of order zero [1,6]. Inspired by their work, we, in this report, show by numerical simulations that in the dc-ac fields, the detection of time-integrated squared THz signals not only can be used to probe the dc-ac induced dynamic localization but also be employed to probe the photon-assisted transport in the presence of excitonic interactions in the coherent regime.

We begin with the following semiconductor Bloch equations by including the longitudinal external driving fields $\mathbf{F}(t)$:

$$\left[\frac{\partial}{\partial t} - \frac{e}{\hbar} \mathbf{F}(t) \cdot \nabla_{\mathbf{k}} - \frac{i}{\hbar} [e_c(\mathbf{k}, t) - e_v(\mathbf{k}, t)] \right] P(\mathbf{k}, t) = \frac{i}{\hbar} [n_c(\mathbf{k}, t) - n_v(\mathbf{k}, t)] \Omega(\mathbf{k}, t) + \left. \frac{\partial P(\mathbf{k}, t)}{\partial t} \right|_{\text{coll}}, \quad (1)$$

$$\left[\frac{\partial}{\partial t} - \frac{e}{\hbar} \mathbf{F}(t) \cdot \nabla_{\mathbf{k}} \right] n_{c,(v)}(\mathbf{k}, t) = \mp \frac{2}{\hbar} \text{Im}[\Omega(\mathbf{k}, t) P^*(\mathbf{k}, t)] + \left. \frac{\partial n_{c,(v)}(\mathbf{k}, t)}{\partial t} \right|_{\text{coll}}. \quad (2)$$

In the above equations, $n_c(\mathbf{k}, t)$ and $n_v(\mathbf{k}, t)$ are the populations in the conduction and valence bands respectively. $P(\mathbf{k}, t)$ is the interband polarization. $e_{c,(v)}(\mathbf{k}, t) = \epsilon_{c,(v)}(\mathbf{k}, t) - \sum_{\mathbf{k}'} V(\mathbf{k}, \mathbf{k}') n_{c,(v)}(\mathbf{k}', t)$ are the electron and hole energies by taking into account of the excitonic interaction, while, $\epsilon_{c,(v)}(\mathbf{k}, t)$ are the corresponding energies of the conduction and (valence) bands with no Coulomb interaction. $\Omega(\mathbf{k}, t) = \mu E(t) + \sum_{\mathbf{k}'} V(\mathbf{k}, \mathbf{k}') P(\mathbf{k}', t)$ is the renormalized Rabi frequency and $V(\mathbf{k}, \mathbf{k}')$ is the Coulomb potential in the quasi-momentum space. $E(t)$ is the optical field and assumed to be the Gaussian laser pulses [6]. $\mathbf{F}(t)$ is the combined dc-ac fields: $\mathbf{F}(t) = \mathbf{F}_0 + \mathbf{F}_1 \cos(\omega t)$. Incoherent dissipative processes are phenomenologically described by the last terms in Eqs. (1) and (2).

If the energy quanta of the optical field $E(t)$ is off resonant with the excitonic resonance, the low excitation regime can be produced. In this regime, the perturbation expansion of Eqs. (1) and (2) according to the optical field can be performed by the following procedure [6,7]: $n_{c,(v)}(\mathbf{k}, t) = n_{c,(v)}^{(0)}(\mathbf{k}, t) + n_{c,(v)}^{(2)}(\mathbf{k}, t) + \dots$; $P(\mathbf{k}, t) = P^{(1)}(\mathbf{k}, t) + P^{(3)}(\mathbf{k}, t) + \dots$. The usual initial condition that SL is in the ground state before the optical pulse is triggered is adopted, i.e., $n_v(\mathbf{k}, t=0) = 1.0$, $n_c(\mathbf{k}, t=0) = 0$. Up to the second-order in the optical field, we can get the partial differential equations for both the first-order interband polarization $P^{(1)}(\mathbf{k}, t)$ and the second-order electron (hole) population density $n_{c,(v)}^{(2)}(\mathbf{k}, t)$ [6].

For simplicity, we focus on the 1-D case, which is just the SL growth direction (assumed to be z direction). The driving dc-ac field is assumed to be along this direction, and we adopt the contact Coulomb potential $V\delta(z-z')$, which carries the most important excitonic characteristic [8]. Under the above assumptions, the partial differential equations for the first order $P^{(1)}(k, t)$ and the second order $n^{(2)}(k, t)$ [6] can be reduced to the following integro-differential equations with the help of the accelerated basis in the quasi-momentum k : (by changing k to $k - \eta(t)$, and $\eta(t)$ is defined as: $\eta(t) = \frac{e}{\hbar} \int_0^t F(t') dt'$) [9].

$$\begin{aligned} & \left[\frac{\partial}{\partial t} - \frac{i}{\hbar} [\epsilon_c(k - \eta(t), t) - \epsilon_v(k - \eta(t), t) + V] \right] \tilde{P}^{(1)}(k, t) \\ & = -\frac{i}{\hbar} \left[\mu E(t) + V \sum_q \tilde{P}^{(1)}(q, t) \right] - \frac{\tilde{P}^{(1)}(k, t)}{T_1}, \end{aligned} \quad (3)$$

$$\frac{\partial \tilde{n}_{c,(v)}^{(2)}(k, t)}{\partial t} = \mp \frac{2}{\hbar} \text{Im} \left[\left(\mu E(t) + V \sum_q \tilde{P}^{(1)}(q, t) \right) \tilde{P}^{(1)*}(k, t) \right] - \frac{\tilde{n}_{c,(v)}^{(2)}(k, t)}{T_2}, \quad (4)$$

where we have introduced the following new notations for convenience:

$$\tilde{P}^{(1)}(k, t) = P^{(1)}(k - \eta(t), t), \quad \tilde{n}_{c,(v)}^{(2)}(k, t) = n_{c,(v)}^{(2)}(k - \eta(t), t). \quad (5)$$

In Eqs. (3) and (4), we adopt the relaxation approximation by introducing the transverse time T_1 and longitudinal relaxation time T_2 respectively to replace the collision terms. More sophisticated description of these dephasing processes calls for Monte Carlo simulation [10].

As we have mentioned previously, what we want to do is to calculate the time-integrated squared THz signal. The THz emission signal in SL can be expressed as $S_{\text{THz}}(t) \propto \partial_t j^{(2)}(t)$, where $j^{(2)}(t) = \frac{e}{\hbar} \sum_i \int \partial \epsilon_i(k) / \partial k n_i^{(2)}(k, t) dk$ ($i = c, v$) is the current due to the non-equilibrium distribution of electrons and holes excited by the Gaussian laser pulses. This current can be rewritten in the following equivalent form with the help of accelerated basis

$$j^{(2)}(t) = \frac{e}{\hbar} \sum_i \int \frac{\partial \epsilon_i(k - \eta(t))}{\partial k} \tilde{n}_i^{(2)}(k, t) dk \quad (i = c, v) . \quad (6)$$

Solving Eqs. (3) and (4) in the accelerated basis in k space is more convenient than the direct integration in the usual quasi-momentum space. In the following numerical simulation, we use the similar parameters as those used by T. Meier *et al.* The combined miniband width $\Delta = \Delta_c + \Delta_v = 20$ meV (here, we use the tight-binding model as in Ref.[6]); Coulomb potential strength $V=10$ meV. The central frequency of the optical field is assumed to be located at 2meV below excitonic resonance which satisfies the off-resonant condition [11]. The full width at half maximum of Gaussian laser pulse envelope $|E(t)|^2$ is chosen to be 100 fs. Both transverse and longitudinal relaxation time T_1 and T_2 have been set to be 2 ps. The energy quanta of the ac field $\hbar\omega$ is fixed to be 20 meV. To capture the information on dynamic localization, we set the ratio of the Stark frequency ω_B to the ac field frequency ω to be an integer, e.g, $n = 1$, without loss of generality. We change the ratio $eF_1d/\hbar\omega$ continuously, and monitor the time-integrated squared THz emission signal through the calculation of the following quantity:

$$T_s \propto \int d\tau |S_{\text{THz}}(\tau)|^2 . \quad (7)$$

The plot of the time-integrated THz signal vs. the ratio $eF_1d/\hbar\omega$ has been shown in Fig.1. In this figure, it can be clearly seen that when the ratio $eF_1d/\hbar\omega$ scans through 3.95, 6.95, 10.0, which are approximately the roots of the ordinary Bessel function of the first order J_1 , the time-integrated squared signal falls into valleys. While the peaks in the plot lies in the vicinity at those values of $eF_1d/\hbar\omega$ that make $|J_1(eF_1d/\hbar\omega)|^2$ reach the local maxima. From the above effect, it is obvious that $|J_1(eF_1d/\hbar\omega)|^2$ reflects the signal T_s profile qualitatively. All the above phenomena demonstrate that even in the presence of Coulomb excitonic interaction whose strength is comparable to the miniband widths of SL, dc-ac induced dynamic localization still appears. This kind of dynamic localization can be probed through the observation of the signal T_s just like the case of a pure ac field [6].

Another aspect of the combined dc-ac fields on the transport of the SL lies in that electrons/holes can tunnel through the adjacent wells through the photon emission and absorption, when the ratio of the Stark frequency of dc field ω_B to the ac field frequency ω is an integer [3]. This phenomenon is the so-called *inverse Bloch oscillators*, which was found in a recent experimental study by Unterrainer et al in the static regime [4]. The coherent regime counterpart of this effect can also be found in our numerical calculation, which was shown in Fig.2. In this figure, we give the plot of the time-integrated squared THz emission signal vs. the ratio ω_B/ω , and set the ratio $eF_1d/\hbar\omega$ to be 2.0. From the figure, we can see that the large peaks appear at the location where the ratio ω_B/ω is an integer. The other distinctive peaks, which appear at fractional ω_B/ω can be attributed to the dynamical fractional Wannier-Stark ladders theoretically proposed recently [5,12].

Let us look at the competition effect between the dc-ac induced dynamic localization and the photon-assisted transport facilitated by coupling of the combined dc-ac fields. The competition between these two effects is shown in Fig.3, where we show the plot of the time-integrated squared THz emission signals vs. the ratio ω_B/ω . In this figure, we set the ratio $eF_1d/\hbar\omega$ to be around 3.8 which is the first root of the ordinary Bessel function of the first order. It can be clearly seen that the signal shows a deep valley when the

ratio ω_B/ω reaches around the unity. While, the peaks appearing at $\omega_B/\omega = 2, 3$ are still present. In other words, the one-photon assisted transport has been suppressed by this specific selection of field parameters, and the dynamic localization prevails over the one-photon assisted transport. If we shift the ratio from those values which are in the vicinity of the roots of the first-order ordinary Bessel function, the one-photon assisted transport can revive. This regeneration can be clearly seen from the Fig.2. We can further suppress the two-photon resonance by selecting the ratio ω_B/ω to be 2, and another ratio $eF_1d/\hbar\omega$ to be the roots of the ordinary Bessel function of the order 2, i.e., make $J_2(eF_1d/\hbar\omega) = 0$, which we don't show for saving space.

In summary, using the tight-binding model driven by dc-ac fields and perturbatively solving the semiconductor Bloch equations in the accelerated quasi-momentum space, we found that the time-integrated squared THz emission signal reveals both the dynamic localization and the multi-photon resonance in the coherent regime. The dynamic localization can be fulfilled when the ratio of Stark frequency ω_B of dc fields to the ac field frequency ω is an integer n , and the another ratio $eF_1d/\hbar\omega$ is located around one of the roots of the n -th order ordinary Bessel function J_n . The dynamic localization is embodied by suppressing the oscillation amplitude of the THz emission signals. Multiphoton assisted transport (resonance) can be identified when time-integrated squared THz emission signals reach peaks provided that the ratio ω_B/ω is an integer, and another ratio $eF_1d/\hbar\omega$ is not in the vicinity of the roots of the ordinary Bessel function of integral order. Otherwise, the photon-assisted transport will be destroyed by the dynamic localization. Experimentally, all the above findings can be probed by detecting the time-integrated squared THz emission signals from the ultra-short laser pulse excited SL driven by combined dc-ac fields. For example, one can use the similar experimental arrangement by the UCSB group [4].

ACKNOWLEDGMENT

The authors thank Dr. T. Meier, Prof. W.-M. Zheng and Prof. J. Liu for the stimulating and useful discussions. This work was supported in part by the National Natural Science Foundations of China under grant No. 19724517, a grant of China Academy of Engineering and Physics, and China Postdoctoral Science foundation.

REFERENCES

- [1] D.H. Dunlap and V.M. Kenkre, Phys. Rev. B **34**, 3625 (1986); A.W. Ghosh, A.V. Kutznetsov, and J.W. Wilkins, Phys. Rev. Lett. **79**, 3494 (1997); X.-G. Zhao, Phys. Lett. A **155**, 299 (1991).
- [2] B.S. Monozon, J.L. Dunn, and C.A. Bates, Phys. Rev. B **50**, 17097 (1994); B.S. Monozon, J.L. Dunn, and C.A. Bates, J. Phys.:Condens. Matter **8**, 877 (1996).
- [3] B.J. Keay, S. Zeuner, S.J. Allen, Jr., K.D. Maranowski, A.C. Gossard, U. Bhattacharya, and M.J.W. Rodwell, Phys. Rev. Lett. **75**, 4102 (1995).
- [4] K. Unterrainer, B.J. Keay, M.C. Wanke, S.J. Allen, D. Leonard, G. Medeiros-Ribeiro, U. Bhattacharya, and M.J. Rodwell, Phys. Rev. Lett. **76**, 2973 (1996), and references therein.
- [5] X.-G. Zhao, R. Jahnke, and Q. Niu, Phys. Lett. A **202**, 297 (1995); X.-G. Zhao, G. A. Georgakis, and Q. Niu, Phys. Rev. B **56**, 3976 (1997); W.-X. Yan, X.-G. Zhao, H. Wang, J. Phys. Condens. Matter (in press).
- [6] T. Meier, G. von Plessen, and P. Thomas, Phys. Rev. Lett. **73**, 902 (1994); Phys. Rev. B **51**, 14490 (1995) and references therein.
- [7] Y.R. Shen, *The principles of nonlinear optics* (John Wiley and Sons, New York, 1984), P.9.
- [8] S. Schmitt-Rink, D.S. Chemla, W.H. Knox, and D.A.B. Miller, Opt. Lett. **15**, 60 (1990).
- [9] W. Quade, E. Schöll, F. Rossi, and C. Jacoboni, Phys. Rev. B **50**, 7389 (1994).
- [10] T. Kuhn and F. Rossi, Phys. Rev. Lett. **69**, 977 (1992); T. Meier, F. Rossi, P. Thomas, and S.W. Koch, Phys. Rev. Lett. **75**, 2558 (1995).
- [11] T. Meier (private communication), the excitonic resonance is determined from the flat band condition.
- [12] Q. Niu, X.-G. Zhao, G.A. Georgakis, M.G. Raizen, Phys. Rev. Lett. **76**, 4504 (1996).

FIGURES

FIG. 1. The plot of time-integrated squared THz emission signal vs. the ratio $eF_1d/\hbar\omega$, showing the dynamic localization induced by dc-ac fields. The parameters used in this figure are declared in the text.

FIG. 2. The plot of time-integrated squared THz emission signal vs. the ratio ω_B/ω , multi-photon resonance can be clearly seen. We choose the ratio $eF_1d/\hbar\omega$ to be 2.0, which is well away from the roots of the first-order ordinary Bessel function.

FIG. 3. The same plot as that of Fig.2, but we choose the ratio $eF_1d/\hbar\omega$ to be 3.8, which is around the root of the first-order ordinary Bessel functions.

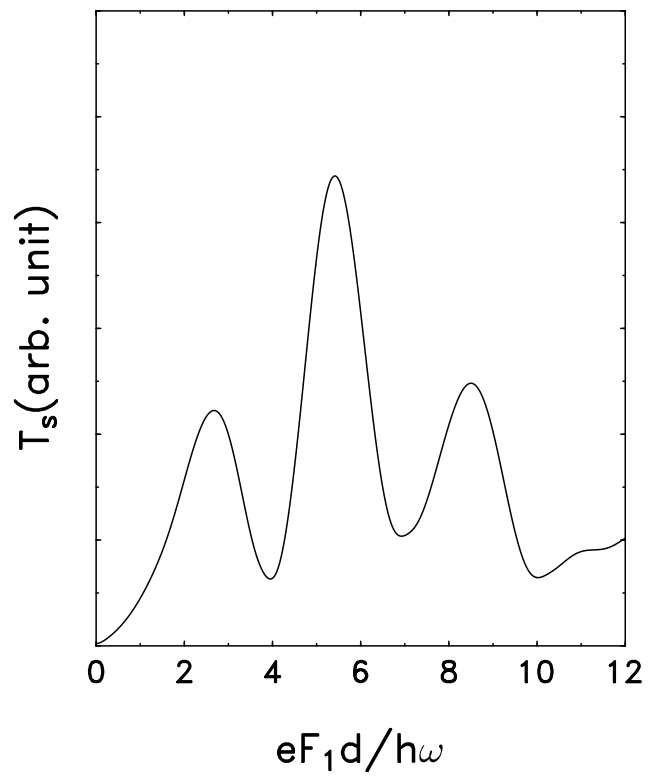


Fig. 1

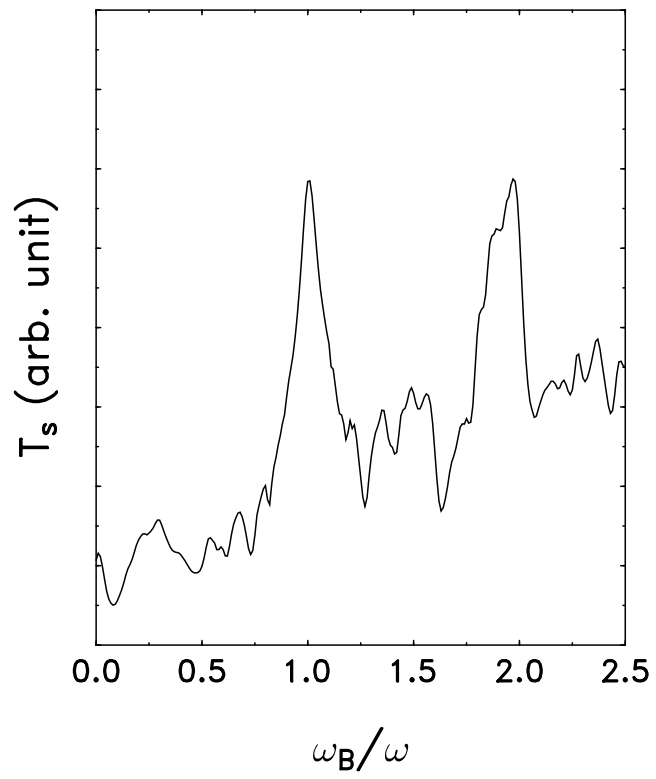


Fig. 2

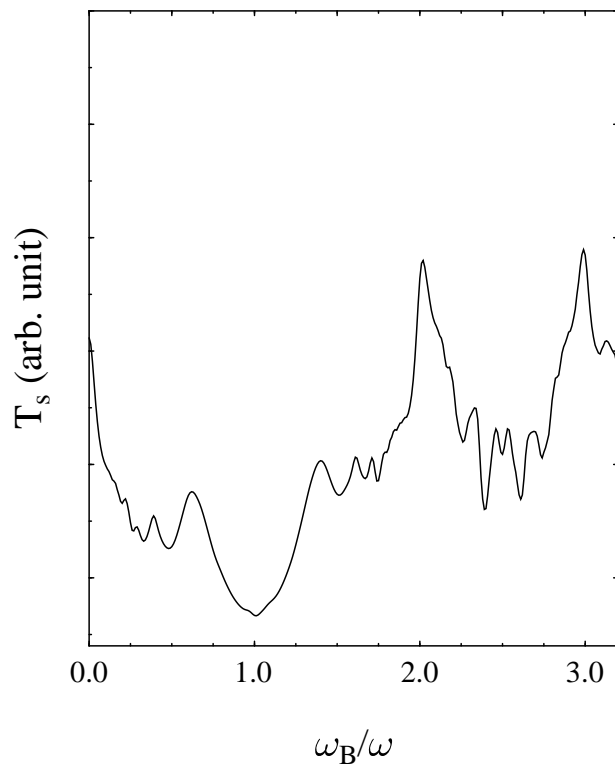


Fig. 3